Communication: Identification of daughter ions through their electronic spectroscopy at low temperature

Claude Dedonder, Géraldine Féraud, Christophe Jouvet

Communication: Identification of daughter ions through their electronic spectroscopy at low temperature

Claude Dedonder, Géraldine Féraud, and Christophe Jouvet*,

Aix-Marseille Université, CNRS, PIIM, UMR-7345, Marseille Cedex 20, France
*christophe.jouvet@univ-amu.fr

Abstract

We present experimental results on photofragmentation of cold fragments issued from the photofragmentation of a cold parent ion. The cooling of the daughter ion at a few K allows its characterization not only through its fragmentation pattern but also through its well resolved electronic spectroscopy. This method is demonstrated on the photofragment resulting from the Cα-Cβ bond rupture of protonated tyrosine. The analysis of the daughter ion (m/z 108) photofragmentation spectrum seems to be in agreement with the mechanism implying a proton transfer to the phenyl ring as the first step of the fragmentation mechanism of protonated tyrosine.

Introduction

Identification of ions often relies on MS^2 fragmentation, a standard technique in mass spectrometry, which consists in isolation of parent ions of given m/z in the mass spectrometer then collision induced dissociation (CID), isolation of a particular fragment and CID of this fragment. The CID fragments can also be characterized by spectroscopic techniques, as shown for benzylium ions produced from CID of protonated benzylamine.[1,2]

UV optical excitation is another way of fragmenting ions and the electronic structure of the parent ion gives information on the ion structure. The daughter ion can be further characterized using photofragmentation in the IR or the UV. Such experiments have been recently performed using a combination in both UV/visible[3,4] and UV/IRMPD[5] method. If the overall nature of the ion has been obtained, the precise knowledge of the tautomeric form (for example) cannot be obtained from such experiments due to the spectral congestion. Moreover, in the IRMPD experiment, the identification of the tautomers is strongly dependant on the IRMPD dissociation yield which is a non-linear process and thus the intensities of the bands are not reliable[6].

We propose a method to characterize the isomeric structure of the ionic photo-product. The first step is the photofragmentation of the selected cold ion parent, the second step is to cool down the daughter ion at low temperature and further photofragment it. With a cold fragment, the spectroscopy can be well resolved and precise information on the nature of the ion fragment can be gained.

We choose the case of protonated tyrosine in which the C_α-C_β bond is dissociated upon optical excitation, this channel being specific of the UV excitation.[7,8,9] This is a key mechanism for studying electronic photofragmentation of very large peptides, which break only if this channel is open. Indeed in very large peptides, if the initial energy brought by the photon is converted in ground state vibrations, the statistical fragmentation can be too long to be observed.

In the isolated protonated aromatic amino acids, the proton is selectively located on the amino group[10,11]. When protonated tryptophan (Trp) is excited at 266 nm, the C_α-C_β bond rupture leads to 3 fragments of m/z 130, 131 and 132.[9,12-16] The first one corresponds to the simple dissociation of the C_α-C_β bond, the second one to the rupture with the transfer of one proton to the indole ring and the third one to the transfer of one proton and one hydrogen. For the simple dissociation of the C_α-C_β bond (m/z 130), two fragmentation times have been evidenced, one in the ns range and another in the ms range,[9] corresponding to two totally different mechanisms. Thus, this bond dissociation, which is specific of the electronic excitation, is not a simple mechanism. In protonated tyrosine, the simple C_α-C_β bond rupture should lead to the m/z 107 fragment but the fragment observed when the first electronic state is excited is m/z 108.[17] Thus one proton is transferred to the daughter ion. Where on the daughter ion is the proton attached (see Figure **1**): on the substituent, giving the cresol ion, or on the phenol ring? This knowledge can help to understand the fragmentation mechanism of the parent ion. One can propose that the m/z 108 fragment is produced by dissociation of the C_α-C_β bond followed by a proton transfer to the cycle after the bond dissociation in the collision complex. This reaction occurring in the ground state (statistical fragmentation), the m/z 108 photofragment should take the most stable form i.e. the cresol cation (Fig. 1).

On the other hand, ab-initio calculations indicate that a proton transfer from the protonated amino group to the phenolic ring (in the C3 or C5 position) can be the first step of the C_α-C_β dissociation and that the C_α-C_β bond is breaking without further rearrangement.[18] If there is no statistical scrambling, the proton should stay on the initial carbon atom of the phenol ring. The ground state of this structure is quite high in energy as compared to that of the cresol cation (1 eV).

Can we discriminate between the two structures of the m/z 108 fragment of protonated tyrosine, namely the cresol ion (the most stable structure), and the species in which the proton is attached to the phenol ring (direct product formed by proton transfer)? This paper is meant to answer this question.

The role of the triplet state in the fragmentation process has been evidenced in the ethylbenzene case.[19] If it is a main reactive channel, a delay between the excitation of the ion and the formation of the product should be observed. This will be investigated with a two-color pump-probe experiment, giving access to the time of appearance of the photofragment coming from the C_α-C_β bond rupture.

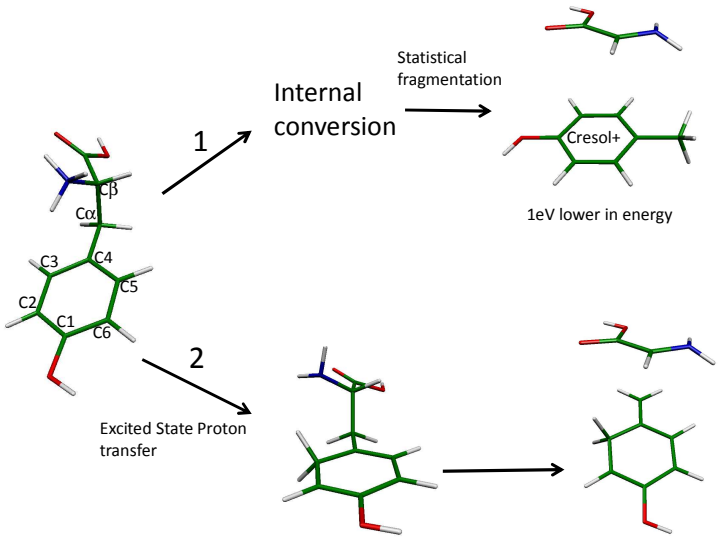

Figure 1 : scheme of the possible fragmentation mechanisms for the **C_α-C_β** bond rupture. In channel 1, the fragmentation occurs through statistical fragmentation in the ground state, leading to the most stable fragment, cresol$^+$. For channel 2, the

fragmentation occurs after proton transfer to the phenolic ring and the proton stays on the cycle. The ground state of cresol$^+$ is 1 eV lower in energy than that of the cation with the proton on the phenolic ring.

Experiment

The experimental setup has been described in previous publications.[20,21] The setup is composed of 3 parts; an electrospray ion source (ESI), a cold ion-trap (CIT) and a time-of-flight mass spectrometer (TOF-Mass). Protonated ions are produced in the ESI source[22] and, at the exit of the capillary, are trapped in an octupole trap for 90 ms. They are extracted by applying a negative pulse and further accelerated by a second pulsed voltage just after the exit electrode. This time sequence produces ion packets with 500 ns - 1 µs duration. The ions are driven byelectrostatic lenses toward the Paul trap biased at 190 V. A mass gate at the entrance of the trap allows selecting the parent ion. The ions are trapped at 10 Hz in the Paul trap cooled by a cryostat and filled with helium buffer gas injected with a pulsed valve[23] operating at 20 Hz, so there are two He pulses in a trapping event. The ions are thermalized at a temperature around 30 K while they stay in the trap. After 49 ms, the pump UV laser is triggered to dissociate the cold parent ions. 1ms after the pump laser, the trap is filled up with a second pulse of He to cool down the photoproduct ions. The second laser probing the fragments (and the remaining parent ions) is sent 40 ms after the second He pulse so that the fragments have enough time to cool down ("cold fragments"). All the ions are extracted from the trap a few µs after the second laser pulse and are detected on a microchannel plates detector (MCP).

The "hot fragments" were also studied, with the valve functioning at 10 Hz and with the second laser fired 1 ms after the first laser. For the two-color pump-probe lifetime experiment, the delay between the pump and the probe laser beams was varied electronically and the depopulation/appearance of the fragments were recorded.

The two lasers are OPO lasers (EKSPLA model-NT342B), which operate at 10 Hz repetition rate. They have a spectral resolution of 8 cm^{-1} and a scanning step of 0.02 nm. The lasers are shaped to a 2 mm^2 spot in the trap and the laser power is around 5 mW.

Results and discussion

The spectrum of protonated tyrosine in a cold trap has been reported previously.[17,24-26] It presents four conformers but, with our laser resolution, it is difficult to clearly separate the different conformers. The pump laser is set at 283.6 nm which is the most intense band in the low energy UV region in which the m/z 108 fragment yield is largely dominent. It has been shown that at higher energy, some other channels open:[17] the fragmentation mechanism in the excited state of protonated tyrosine is quite complex.

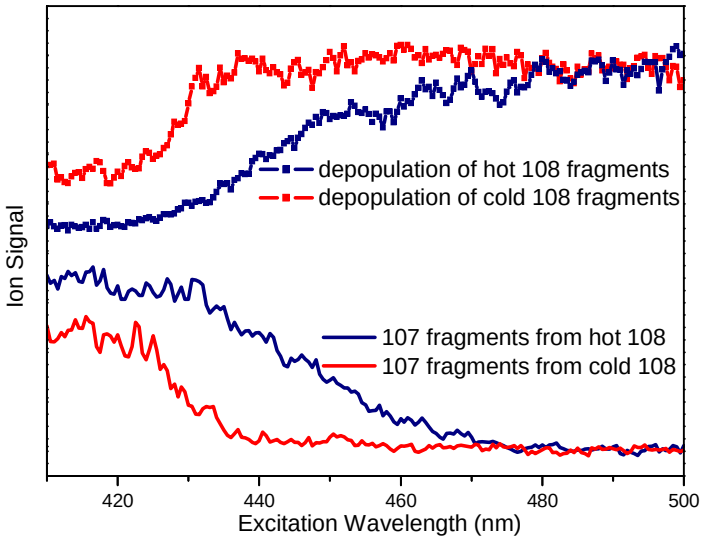

Figure 2: Photofragmentation spectrum of the m /z 108 fragment issued from the photofragmentation of protonated tyrosine excited at 283.6 nm. In blue, hot m/z 108 ions directly issued from tyrosineH^+ are fragmented. In red, the m/z 108 fragment is cooled down before its fragmentation. Photofragmentation of the m/z 108 fragment leads only to H loss (m/z 107). These spectra were recorded with a 0.5 nm scanning step.

In Figure **2** are presented the spectra of depopulation of the fragment ion (m/z 108) (daughter ion of protonated tyrosine) and the appearance of the m/z 107 fragment ion (grand-daughter ion of protonated tyrosine and daughter ion of m/z 108) as a function of the probe laser wavelength in two experimental conditions. There is a clear correlation between the depopulation of the m/z 108 fragment and the appearance of the m/z 107 fragments. For the m/z 108 fragment, the first absorption band is observed at around 440 nm (the laser has been scanned up to 700 nm i.e. 1.77 eV and there are no other bands). Upon this absorption, the ion is fragmenting losing an H atom leading to the m/z 107 fragment. For the blue spectra, the probe laser is fired 1 ms after the pump laser, i.e. the m/z 108 fragment is not relaxed and the onset of the absorption band is quite broad indicating a warm ion. At the opposite when the probe laser is applied after the cooling He pulse (red spectra), the fragment is quite cold and the onset of the spectrum becomes more abrupt and blue shifted as expected for a cold molecule. As a matter of fact, in similar experimental conditions benzylium ions produced from photo-fragmentation of protonated benzylamine[1,2] do not exhibit hot bands indicating that the product ion temperature is quite cold (around 30 K) as for the parent ion.

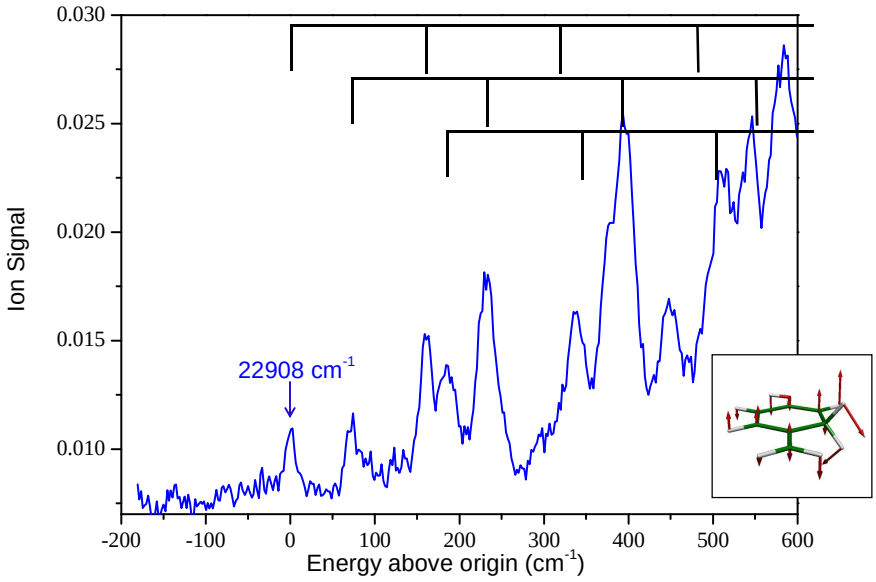

Figure 3 : close up of the photofragmentation spectrum of the cold m /z 108 fragment near the S_1-S_0 band origin. The m/z 108 fragment is issued from the photofragmentation of protonated tyrosine excited at 283.6 nm. The spectrum is recorded on the m/z 107 photoproduct with a 0.02 nm scanning step. The 160 cm^{-1} active mode is represented in the inset and the vibrational progression is represented on top of the figure.

In Figure 3 is presented the lower energy region of the electronic spectrum of the m/z 108 fragment recorded in detecting the m/z 107 product, with a first band at 22908 cm^{-1} (436.5 nm/2.84 eV**)**. At this scale, a clear vibrational structure is observed, with vibrational bands slightly larger that our experimental resolution (10 cm^{-1}). Vibrational progressions can be followed for a few hundreds of wavenumbers before the spectrum becomes congested. The first transition observed is not the most intense band and the intensity of the vibronic transitions increases as the energy increases, indicating some change in geometry between the ground and excited state, but not a huge change since well separated vibronic bands are observed. Assuming that the first band observed is the origin of the transition, the spectrum can be assigned to progressions on a 160 cm^{-1} mode starting at 0, +71 cm^{-1}, +185 cm^{-1} (see figure 3). The origin transition could be missed by one quantum of the 160 cm^{-1} vibration, but probably not by more than one quantum since a lower transition origin would imply a more congested band system in the vicinity of the first bands observed. The ground state frequencies have been calculated, and 3 low vibrational modes at 94, 203, and 301 cm^{-1} are active. The progression on the 160 cm^{-1} mode in the excited state may correspond to the 203 cm^{-1} ground state out-of-plane mode, and the +71 cm^{-1} band may correspond to the ground state vibration of 94 cm^{-1}.

The assignment of the band system relies on the excited state calculations. Ab-initio calculations were performed with the TURBOMOLE® program package.[27] The system is not a closed shell structure, which leads to convergence problems at the SCF level. We have obtained a consistent set of results using the TD-DFT / b3-lyp method with SV(P) basis set. A few values have been calculated at the ri-adc(2)/cc-pVDZ level and are consistent with the TD-DFT values. Both the vertical and adiabatic excited states energies of S_1 and S_2 states have been calculated.

The results of the calculations for different isomers of m/z 108 are summarized in table 1. C3 and C2 correspond to ions protonated on the C3 or C2 carbon atom of the phenol

ring (see figure 1 for atom numbering) and in these cases the trans conformer has been calculated (as in figure 1).

Table 1: calculations at the B3-LYP/SV(P) level of the ground and excited state energies of different ionic isomers of the m/z 108 photofragment (cresol, C3 and C2). The vertical (vert.) and adiabatic (adia.) energies are given in eV and the oscillator strength (Osc.) in velocity representation. The experimental 0-0 transition is observed at 2.84 eV.

	ground	S1 vert.	S1 adia.	Osc.	S2 vert.	S2 adia.	Osc.
	DFT(MP2)						
Cresol	0 (0)	1.51	1.16	4.52E-04	3.16	2.33	6.11E-02
C3	0.82 (1.18)	2.05	1.99	0.013	2.95	**2.86**	**0.157**
C2	1.01	1.02	1.16	4.21E-03	2.79	2.63	5.61E-05

When considering vertical energies, both the C3 ion and cresol cation can be responsible for the observed electronic transition through a $S_2 \leftarrow S_0$ transition. The C2 can be excluded since the possible transition in the 2.8 eV region has a very weak oscillator strength. After optimization of the first and second excited states, the adiabatic values for the S_2-S_0 and S_1-S_0 transitions have been obtained. The agreement between the adiabatic calculated value of the S_2-S_0 transition and the experimental band origin is quite good (in the energetical point of view) for the C3 isomer and the oscillator strength is also quite favorable. For the cresol ion, the difference between adiabatic calculated and experimental transition energies (experiment-theory=0.51eV) is much larger than the usual uncertainty for the adiabatic values, typically less than 0.2 eV. Moreover in the S_2 state optimization of the cresol ion, the hydrogen atom of the hydroxyl group, which is in the plane of the aromatic ring in the ground state, flips to a perpendicular position in the excited state, which implies a very bad Franck Condon factor to the 0-0 transition. To the extent that open shell excited state calculations can be trusted, one can then assign the observed m/z 108 fragment to the species with the proton on the C3 carbon of the aromatic ring.

The cis conformer of the C3 isomer has been calculated to be 60 cm^{-1} less stable than the trans conformer in the ground state and its S_0-S_1 transition is expected to be shifted by +170 cm^{-1}. We tentatively assign the second band at +185 cm^{-1} to the cis isomer.

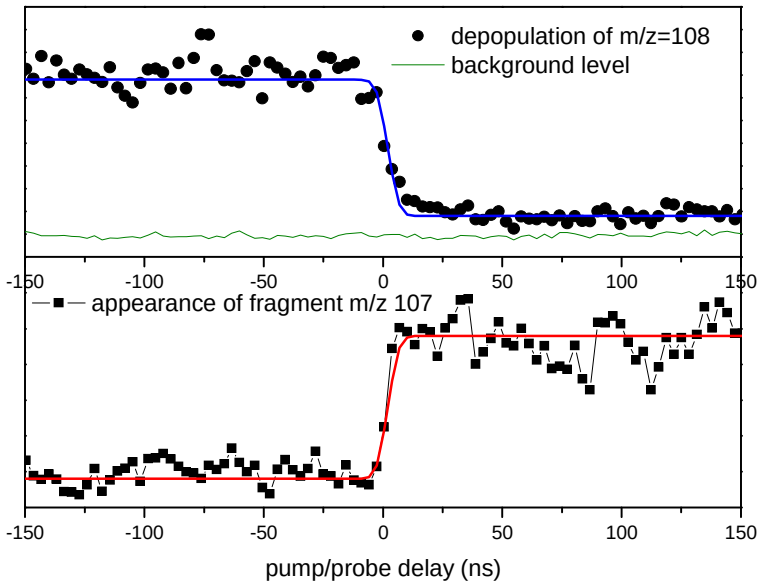

Figure 4 Pump-probe signals: disappearance of m/z 108 fragment (black circles in the upper panel) and appearance of m/z 107 fragment (black squares in the lower panel). Fitting functions are plotted in blue (upper panel) and red (lower panel). In the upper panel, the pump probe signal is compared with the background level (thin line) obtained with the probe only.

Figure 4 represents the signal from the pump-probe experiment. The pump laser is fixed at 283.6 nm and the probe laser at 420 nm. The delay between the two lasers is scanned during 300 ns. The pump laser produces the m/z 108 ion and the probe laser the m/z 107 ion. The depopulation of the m/z 108 photofragment and the appearance of its m/z 107 photofragment occur in ~20 ns, i.e. it is in the same order of magnitude as the cross-correlation function of the lasers. In other words, the fragmentation time of m/z 108 photofragment is very short, and its formation from protonated tyrosine is also very rapid. A small fraction of the m/z 108 ions (~10%) remains with respect to the background level that could be formed from the triplet state but is most probably due to fragmentation efficiency, which is certainly less than 100%. So the pump-probe experiment indicates mainly short time scales for the fragmentation of the C_α-C_β bond in protonated tyrosine alone, a small contribution of longer time scales cannot be ruled out but is certainly very minor.

Conclusions

We have shown here that using a cold ion trap and a combination of He pulses one can cool down the photodissociation products well enough to get a clean spectroscopy of the photofragment. In the case of protonated tyrosine photofragmentation, theoretical calculations were predicting a proton transfer from the amino group to the phenyl ring as a necessary step to induce the C_α-C_β bond rupture. The present experiment seems to validate this mechanism, in the accuracy limits of excited state UHF calculations.

Acknowledgments

This works was supported by the Aix-Marseille Université, the ANR Research Grant (ANR2010BLANC040501_ESPEM). We acknowledge the use of the computing facility cluster GMPCS of the LUMAT federation (FR LUMAT 2764).

References

1. Féraud G, Dedonder-lardeux C, Soorkia S, Jouvet C. Photo-fragmentation spectroscopy of benzylium and 1-phenylethyl cations. *J Chem Phys*. 2014;024302:1-10. doi:10.1063/1.4858409.

2. Féraud G, Broquier M, Dedonder-Lardeux C, Grégoire G, Soorkia S, Jouvet C. Photofragmentation Spectroscopy of Cold Protonated Aromatic Amines in the Gas Phase. *Phys Chem Chem Phys*. 2014;16:5250-5259. doi:10.1039/c3cp54736a.

3. Joly L, Antoine R, Allouche A-R, Dugourd P. Formation and spectroscopy of a tryptophan radical containing peptide in the gas phase. *J Am Chem Soc*. 2008;130(42):13832-3. doi:10.1021/ja804508d.

4. Useli-Bacchitta F, Bonnamy A, Mulas G, Malloci G, Toublanc D, Joblin C. Visible photodissociation spectroscopy of PAH cations and derivatives in the PIRENEA experiment. *Chemical Physics*. 2010;371(1-3):16-23.

5. Scuderi D, Lepere V, Piani G, Bouchet A, Zehnacker-Rentien A. Structural Characterization of the UV-Induced Fragmentation Products in an Ion Trap by Infrared Multiple Photon Dissociation Spectroscopy. *The Journal of Physical Chemistry Letters*. 2014;5(1):56-61. doi:10.1021/jz402348n.

6. Škríba A, Janková Š, Váňa J, et al. Protonation Sites and Fragmentations of Para-aminophenol. *International Journal of Mass Spectrometry*. 2013;337:18-23. doi:10.1016/j.ijms.2012.12.007.

7. Svendsen A, Lorenz UJ, Boyarkin OV, Rizzo TR. A new tandem mass spectrometer for photofragment spectroscopy of cold gas-phase molecular ions. *Rev Sci Instrum*. 2010;81:073107.

8. Rizzo TR, Stearns JA, Boyarkin OV. Spectroscopic studies of cold, gas-phase biomolecular ions. *Int Rev Phys Chem*. 2009;28(3):481-515. doi:10.1080/01442350903069931.

9. Lucas B, Barat M, Fayeton JA, et al. Mechanisms of photoinduced C-alpha-C-beta bond breakage in protonated aromatic amino acids. *J Chem Phys*. 2008;128(16):164302. Available at: http://apps.isiknowledge.com/full_record.do?product=WOS&search_mode=GeneralSearch&qid=1&SID=Q2kmNlkOKMC8G1MNcjH&page=1&doc=15. Accessed September 2, 2010.

10. Maksic ZB, Kovacevic B. No Title. *Chem Phys Lett*. 1999;307:497.

11. Lioe H, O'Hair RAJ, Reid GE. Gas phase ion Chem. biomolecules. Part 37 - Gas-phase reactions of protonated tryptophan. *J Am Soc Mass Spectrom*. 2004;15(1):65-76. Available at: <Go to ISI>://000187940400009.

12. Kang H, Dedonder-Lardeux C, Jouvet C, et al. Photo-induced dissociation of protonated tryptophan TrpH+: A direct dissociation channel in the excited states controls the hydrogen atom loss. *Phys Chem Chem Phys*. 2004;6(10):2628-2632. doi:10.1039/b315425d.

13. Kang H, Dedonder-Lardeux C, Jouvet C, et al. Control of Bond-cleaving Reactions of Free Protonated Tryptophan Ion by Femtosecond Laser Pulses. *J Phys Chem A*. 2005;109(11):2417-2420. doi:10.1021/jp0407167.

14. Kang H, Jouvet C, Dedonder-Lardeux C, et al. Ultrafast Deactivation Mechanisms of Protonated Aromatic Amino Acids Following UV Excitation. *Phys Chem Chem Phys*. 2005;7(2):394-398. Available at: <Go to ISI>://000225888400022 .

15. Grégoire G, Lucas B, Barat M, Fayeton JA, Dedonder-Lardeux C, Jouvet C. UV Photoinduced Dynamics in Protonated Aromatic Amino Acid. *Eur Phys J D*. 2009;51(1):109-116. doi:10.1140/epjd/e2008-00085-3.

16. Talbot FO, Tabarin T, Antoine R, Broyer M, Dugourd P. Photodissociation spectroscopy of trapped protonated tryptophan. *J Chem Phys*. 2005;122(7):074310. doi:10.1063/1.1850459.

17. Dedonder C, Féraud G, Jouvet C. Excited-State Dynamics of Protonated Aromatic Amino Acids. In: Brøndsted Nielsen S, Wyer JA, eds. *Photophysics of Ionic Biochromophores*. Berlin, Heidelberg: Springer Berlin Heidelberg; 2013:155-180. doi:10.1007/978-3-642-40190-9.

18. Grégoire G, Jouvet C, Dedonder C, Sobolewski AL. Ab initio study of the excited-state deactivation pathways of protonated tryptophan and tyrosine. *J Am Chem Soc*. 2007;129(19):6223-6231. doi:10.1021/ja069050f.

19. Huang C-L, Jiang J-C, Lee YT, Ni C-K. Photodissociation of ethylbenzene and n-propylbenzene in a molecular beam. *The Journal of Chemical Physics*. 2002;117(15):7034. doi:10.1063/1.1507117.

20. Alata I, Bert J, Broquier M, et al. Electronic Spectra of the Protonated Indole Chromophore in the Gas Phase. *The journal of physical chemistry A*. 2013;117(21):4420-7. doi:10.1021/jp402298y.

21. Féraud G, Dedonder C, Jouvet C, et al. Development of Ultraviolet − Ultraviolet Hole-Burning Spectroscopy for Cold Gas-Phase Ions. *J Phys Chem Lett*. 2014;5:1236-1240. doi:10.1021/jz500478w.

22. Andersen JU, Hvelplund P, Nielsen SB, et al. The combination of an electrospray ion source and an electrostatic storage ring for lifetime and spectroscopy experiments on biomolecules. *Rev Sci Instrum*. 2002;73(3):1284. doi:10.1063/1.1447305.

23. Kamrath MZ, Relph RA, Guasco TL, Leavitt CM, Johnson MA. Vibrational Predissociation Spectroscopy of the H2-Tagged Mono- and Dicarboxylate Anions of Dodecanedioic Acid. *Int J Mass Spectrom*. 2011;300(2-3):91-98. doi:10.1016/j.ijms.2010.10.021.

24. Boyarkin OV, Mercier SR, Kamariotis A, Rizzo TR. Electronic Spectroscopy of Cold Protonated Tryptophan and Tyrosine. *J Am Chem Soc*. 2006;128:2816–2817. Available at: 9 .

25. Stearns JA, Mercier S, Seaiby C, Guidi M, Boyarkin OV, Rizzo TR. Conformation-specific spectroscopy and photodissociation of cold, protonated tyrosine and phenylalanine. *J Am Chem Soc*. 2007;129(38):11814-11820. doi:10.1021/ja0736010.

26. Redwine JG, Davis ZS, Burke NL, Oglesbee RA, McLuckey SA, Zwier TS. A Novel Ion Trap Based Tandem Mass Spectrometer for the Spectroscopic Study of Cold Gas Phase Polyatomic Ions. *Int J Mass Spectrom*. 2013;348:9-14.

27. Ahlrichs R, Bär M, Häser M, Horn H, Kölmel C. Electronic Structure Calculations on Workstation Computers: The Program System Turbomole. *Chem Phys Lett*. 1989;162:165-169.